Available online at www.sciencedirect.com
ScienceDirect
Journal of Colloid and Interface Science 304 (2006) 431–436
Journal of Colloid and Interface Science
www.elsevier.com/locate/jcis

Metal-cation-mediated nanocrystal arrays of sandwich-type (phthalocyaninato) [tetrakis(4-pyridyl)porphyrinato] cerium complex formed at the water–chloroform interface

Qingyun Liu [a], Yongzhong Bian [a], Hongguo Liu [a], Xueying Wang [a], Yanli Chen [a,b], Xiyou Li [a], Jianzhuang Jiang [a,*]

[a] *Key Lab for Colloid and Interface Chemistry of Education Ministry, Department of Chemistry, Shandong University, Jinan 250100, China*
[b] *College of Chemistry and Chemical Engineering, Jinan University, Jinan 250022, China*

Received 21 July 2006; accepted 5 September 2006

Abstract

Regular square, wirelike, quadrate, and rodlike nanocrystal arrays of Cd^{2+}, Hg^{2+}, or Ag^{+} metal-cation-mediated sandwich-type mixed (phthalocyaninato) [5,10,15,20-tetrakis(4-pyridyl)poprhyrinato] cerium(III) double-decker complex Ce(Pc)(TPyP) have been successfully prepared at the water–chloroform interface. The nanocrystal growth processes were monitored by transmission electron microscopy (TEM), which reveals that different morphologies of nanocrystals have been fabricated from double-decker molecules connected by different kinds of metal cations, forming coordination polymers. These nanoscaled coordination polymers were characterized by FT-IR spectra and energy-dispersive X-ray spectra (EDS). EDS results clearly revealed the elements of the nanocrystals and the FT-IR spectra give evidence for the coordination interaction between the double-decker molecules and metal cations. The UV–vis absorption spectrum indicates the formation of J-aggregates of the double-decker molecules in the nanocrystals formed.

Keywords: Phthalocyanine; Porphyrin; Cerium; Sandwich complex; Transmission electron microscopy; Nanocrystal

1. Introduction

The self-assembly of molecular building blocks into targeted nanoscaled architectures at interfaces represents one of the major goals of supramolecular chemistry and material science, given the perspective of the potential applications of these systems in nanotechnology [1–4]. On the other hand, the liquid–liquid interface offers great potential for assembly and for the chemical manipulation of nanoparticles [5,6]. The assembly of particles at liquid–liquid interfaces provides a favorable means of preparing various kinds of materials because the particles at the fluid interface are highly mobile and can rapidly achieve an equilibrium assembly [7,8]. For instance, nanoparticles including metal, metal oxide, and metal sulfide [9–12], protein film [13,14], and composite film [15] have been prepared recently at liquid–liquid interfaces.

Supramolecular structures formed from porphyrin derivatives, including phthalocyanines, have received increasing attention recently due to their potential applications, ranging from molecular electronics [16–20], photovoltaic cells [21–23], and field effect transistor (FET) [24–28], to gas sensors [29–33]. The highly ordered supramolecular structures of porphyrin and phthalocyanine derivatives are usually formed in solution driven by noncovalent intermolecular forces such as π–π stacking [34–36], hydrogen bonding [37,38], or metal–ligand bonding [39–41]. Other than the self-assembly of porphyrin and phthalocyanine derivatives in solution, assembly at the immiscible phase interfaces of air–water, air–solid, or liquid–liquid has also attracted much research interest. Most previous research focuses on the self-assembly of porphyrin and/or phthalocyanine derivatives at the air–water interface, which formed various aggregates and assembled into unique functional films [27,28,42–

---

* Corresponding author.
E-mail address: jzjiang@sdu.edu.cn (J. Jiang).

0021-9797/$ – see front matter © 2006 Elsevier Inc. All rights reserved.
doi:10.1016/j.jcis.2006.09.003

44]. Moreover, the self-assembly at the air–solid interface has been successfully used to control the molecular arrangement in two dimensions [45,46]. Recently, metal-mediated multiporphyrin nanocrystals and coordination polymer nanotubes of tetrapyridylporphin compounds have been successfully grown at the water–chloroform interface [47,48].

However, to the best of our knowledge, all the research about metal-mediated multiporphyrin arrays reported thus far seems to be limited to the nanoscale networks of monomeric porphyrin and/or phthalocyanine derivatives. There seems to be no report on the metal-mediated assembly of sandwich-type tetrapyrrole metal complexes at the liquid–liquid interface. Owing to the rich optical and electrochemical properties, as well as the special electronic structure of sandwich-type porphyrinato and/or phthalocyaninato rare earth complexes, it is worth trying to assemble sandwich tetrapyrrole rare earth complexes into supramolecular structures with special functionalities.

Here we describe the self-assembly of a sandwich-type (phthalocyaninato) [tetrakis(4-pyridyl)porphyrinato] cerium double-decker compound, Ce(Pc)(TPyP), driven by metal coordination bonds together with the supramolecular interactions at the water–chloroform interface. The progress of nanocrystal growth of sandwich-type double-decker complexes was monitored by transmission electron microscopy (TEM). In particular, the aggregation of Ce(Pc)(TPyP) mediated by Ag^+ has been found to be concentration-dependent and at least two coordination modes of silver cations with pyridyl nitrogen atoms are formed. This is different from that reported previously [46].

2. Experimental section

2.1. Materials

Sandwich-type (phthalocyaninato)[tetrakis(4-pyridyl)porphyrinato] cerium double-decker compound, Ce(Pc)(TPyP), was prepared following the previously published procedures [19]. $CdCl_2$, $HgCl_2$, and $AgNO_3$ were all analytical grade reagents purchased from the Shanghai Chemical Reagent Co. All chemicals were used as received without further purification. Double distilled water was used to prepare aqueous solutions.

2.2. Nanocrystal growth of Ce(Pc)(TPyP) networks at the water–chloroform interface

A typical procedure for the preparation of Cd^{2+} mediated nanocrystal growth is described below. A 0.036 M $CdCl_2$ water solution and a 0.097 mM Ce(Pc)(TPyP) chloroform solution were used as the water phase and organic phase, respectively. During the experiments, the aqueous solution of metal ions was slowly added to the chloroform phase surface at which the interfacial reaction occurs.

2.3. Characterization of nanocrystals

The TEM images were taken on a JEM-100CX II electron microscope operated at 100 kV (JEOL, Japan). Energy-depressive X-ray spectra (EDS) (OXFORD, UK) were performed on a high-resolution transmission electron microscope (HRTEM) JEM-2100 (JEOL, Japan) operating at 200 KV. FT-IR spectra were recorded on KBr-matrix pellets on a BIORAD FTS-165 spectrometer (PerkinElmer Ltd., UK) with a resolution of 2 cm^{-1}. UV–vis spectra for Ce(Pc)(TPyP) in chloroform solution and the nanocrystal Langmuir–Blodgett (LB) films were measured on a Hitachi U4100 (Japan) UV–vis spectrophotometer.

3. Results and discussion

3.1. Formation of metal-mediated Ce(Pc)(TPyP) network nanocrystals

As noticed by Qian and co-workers [47], the key point for the successful growth of nanocrystals at the water–chloroform interface is that the products do not dissolve into either water or chloroform. Fortunately, we found that the metal cations, namely Cd^{2+}-, Hg^{2+}-, and Ag^+-mediated Ce(Pc)(TPyP) nanocrystals, do not dissolve in either water or chloroform solution. It has also been found that the formation rate of nanocrystals was strongly dependent on the metal cation species: Some fine nanowires of Hg^{2+}-mediated double-decker compound Ce(Pc)(TPyP) could be found in the chloroform phase after 15 min of interfacial reaction when 0.01 M $HgCl_2$ solution was used. In contrast, for the Cd^{2+}-mediated system, 36 h was needed to get regular nanocrystals when $CdCl_2$ (0.039 M) was used.

3.2. TEM images of metal-mediated double-decker nanocrystals

By employing a similar procedure of studying the metal-mediated monomeric porphyrin compounds [47,48], the formation process of nanocrystals of the double-decker compound Ce(Pc)(TPyP) mediated with different metal cations at the water–chloroform interface has been systematically investigated through studying the size and framework of nanocrystals formed as a function of reaction time and concentrations of either metal cations or Ce(Pc)(TPyP) by TEM technology.

3.2.1. Cd-[Ce(Pc)(TPyP)] nanocrystals

Fig. 1 shows a series of TEM images of Cd-[Ce(Pc)(TPyP)] nanocrystals and microcrystals taken at different reaction time. As can be seen from these figures, many nanocrystals with size ca. 200 nm were formed within 1 h, indicating that the reaction at the water–chloroform interface was relatively rapid. Along with increasing the reaction time, the TEM images revealed that the nanocrystals increase gradually in size; for example, crystals with sizes ca. 200–300 nm and 2 μm formed after 2 and 36 h, respectively. It was also found that the nanocrystals formed were not very regular at first, then became regular crystals after 2 h (Fig. 1b), and finally grew into well-defined regular crystals after 36 h (Fig. 1c). Examination of the TEM images seems to reveal that in line with the previous report on metal-mediated monomeric porphyrin compounds [47], the crystals grow not only by the coordination reaction of Cd^{2+} with TPyP

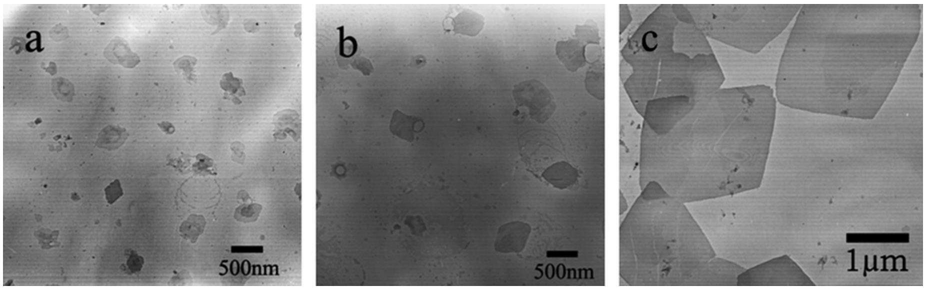

Fig. 1. TEM images of Cd-[Ce(Pc)(TPyP)] nanocrystals grown at the water–chloroform interface after (a) 1 h, (b) 2 h, and (c) 36 h. Concentrations of $CdCl_2$ and Ce(Pc)(TPyP) were 0.036 M and 0.097 mM, respectively.

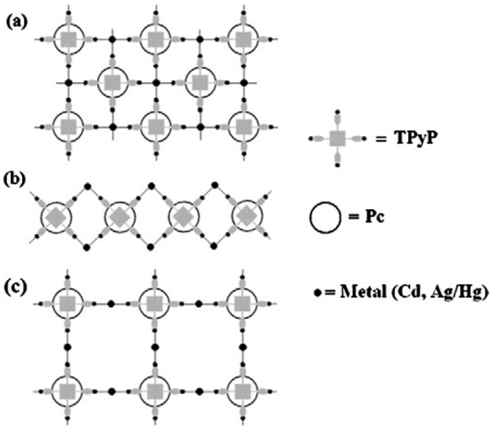

Scheme 1. Three schematic frameworks of metal-cation mediated Ce(Pc)-(TPyP) nanocrystals.

ligand in the double-decker compound Ce(Pc)(TPyP) but also by fusing the neighboring fine crystals formed at beginning. Experimental results also indicate that no significant difference exists in the crystal frameworks by altering the concentration of either $CdCl_2$ (0.005–0.1 M) solution or Ce(Pc)(TPyP) (0.048–0.097 mM). However, the formation speed, the nanocrystal number, and the nanocrytal sizes were found to increase with increasing concentrations of $CdCl_2$ and/or Ce(Pc)(TPyP). It is worth noting that the crystals formed are in the form of ultrathin layers. On the basis of previous results [28,39,42–44,47,48], the framework of Cd-[Ce(Pc)(TPyP)] nanocrystal is formed according to Scheme 1a.

3.2.2. Ag-[Ce(Pc)(TPyP)] nanocrystals

TEM images of the Ag-[Ce(Pc)(TPyP)] nanocrystals in 5 min and 1 h after the interfacial reaction between $AgNO_3$ (0.1 M) and Ce(Pc)(TPyP) (0.097 mM) are shown in Fig. 2. It can be seen that nanorods form very quickly at the interface. The rodlike nanocrystals grow to a size of about 5 nm in width and 400–500 nm in length in 1 h. Further increase in the reaction time after the reaction starts at the interface continuously increases the width and the length of the nanorods due to the bundle formation of the nanorods. The selected electron diffraction for the nanorods formed after 1 h show diffraction circles, indicating the formation of polycrystals.

However, it is interesting to note that regular quadrate nanocrystals form at the water–chloroform interface when the concentration of Ce(Pc)(TPyP) in chloroform decreases to 0.0485 mM. The TEM images of the nanocrystals formed under this experimental condition in 5, 10, and 40 min after the interfacial reaction are shown in Fig. 3. The results show that fine nanocrystals with a size of 10–20 nm were formed within 5 min, Fig. 3a. With increasing reaction time, the size of nanocrystals increases to about 50 nm in 10 min. After 40 min interfacial reaction, regular crystals 1.5 μm in length and 1 μm in width were observed. These TEM images revealed that the nanocrystals were irregular at first and finally grew into regular quadrate crystals. Careful observation of these TEM images also revealed that these regular quadrate crystals were formed by directional aggregation of many smaller globular nanoparticles, Fig. 3 [49–52]. In other words, the regular quadrate nanocrystals are formed not only by coordination reaction of the TPyP ligand in Ce(Pc)(TPyP) with Ag^+ at the water–chloroform interface but also by fusing the neighboring fine crystals. The selected area electron diffraction for the nanocrystals formed after 40 min shows only regular hexagonal diffraction spots, indicating the formation of single crystals.

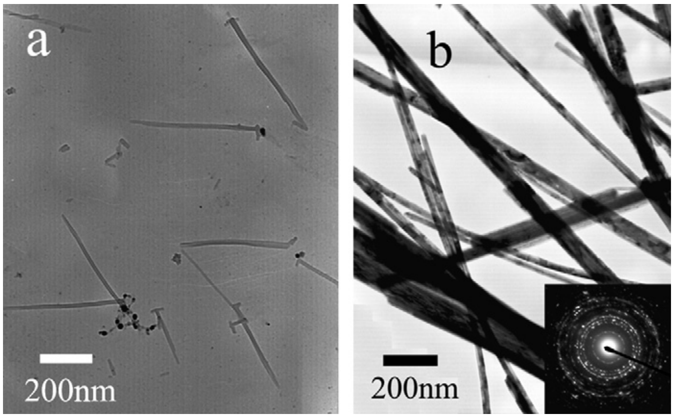

Fig. 2. TEM images of Ag-[Ce(Pc)(TPyP)] nanocrystals grown at the water–chloroform interface after (a) 5 min and (b) 1 h. Concentrations of $AgNO_3$ and Ce(Pc)(TPyP) were 0.1 M and 0.097 mM, respectively. The inset is the corresponding electron diffraction pattern.

The results described above show that the same silver-metal-mediated double-decker compounds can form crystals with different morphologies when the experimental conditions change. This clearly suggests that the crystal morphologies are controlled not only by the metal ion coordination geometry but

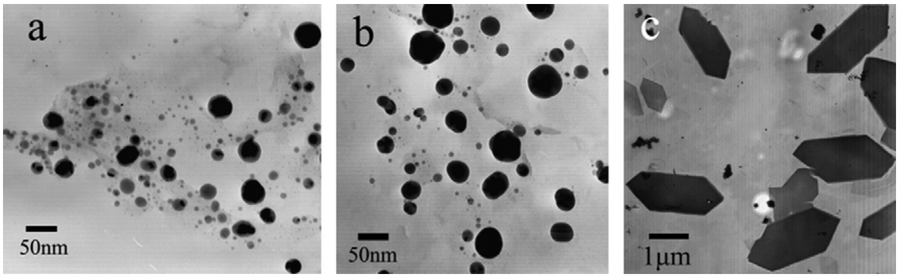

Fig. 3. TEM images of Ag-[Ce(Pc)(TPyP)] nanocrystals grown at the water–chloroform interface after (a) 5 min, (b) 10 min, and (c) 40 min. Concentrations of $AgNO_3$ and Ce(Pc)(TPyP) were 0.1 M and 0.0485 mM, respectively.

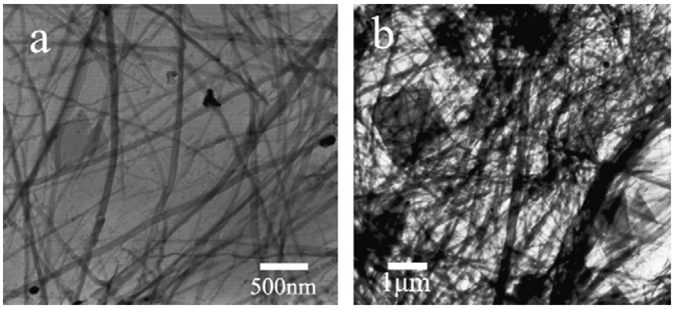

Fig. 4. TEM images of Hg-[Ce(Pc)(TPyP)] nanocrystals grown at the water–chloroform interface. Concentrations of $HgCl_2$ and Ce(Pc)(TPyP) were 0.01 M and 0.097 mM, respectively.

also by the coordination mode of the silver cation with the pyridyl substituents of the double-decker molecules. Since the nanocrystals formed are too small to be analyzed by X-ray crystallographic technique, the coordination mode of the Ag^+ cation with the double-decker molecules can therefore be speculated upon only according to the previous research results, instead of from the definitive structural information. Although silver cation displays versatile coordination geometries in coordination chemistry [40], it appears that the nanorod crystals of the double-decker compound Ce(Pc)(TPyP) mediated by silver cations in the present case might be formed following Scheme 1b [39–41,47,48] and quadrate crystals following Scheme 1c [40].

3.2.3. Hg-[Ce(Pc)(TPyP)] nanocrystals

A similar time dependence feature similar to that of Ag-[Ce(Pc)(TPyP)] nanorods has been revealed for Hg^{2+}-mediated [Ce(Pc)(TPyP)] nanocrystal formation according to the TEM experimental result. As shown in Fig. 4, wirelike nanocrystals formed for Hg-[Ce(Pc)(TPyP)] with a width (diameter) up to about 70–80 nm and a length of several to tens of micrometers, Fig. 4b. Experimental results also indicate that no significant difference of morphologies exists in the crystal frameworks by changing the concentration of either $HgCl_2$ (0.001–0.1 M) solution or Ce(Pc)(TPyP) (0.048–0.097 mM). It can be deduced that the coordination of metal ions in the nanowires adopts a linear geometry, which is common for mercury cations. Each Hg^{2+} binds two adjacent double-decker Ce(Pc)(TPyP) units, while every double-decker entity is linked to four different metal centers, Scheme 1b [39].

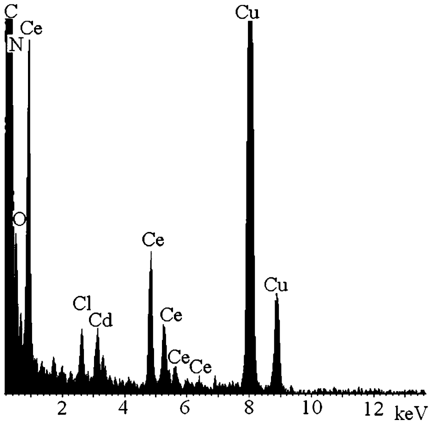

Fig. 5. Energy-dispersive X-ray analysis of Cd–Ce(Pc)(TPyP) nanocrystal.

3.3. EDS analysis

The nanocrystals were deposited on copper grids covered with carbon and measured using HRTEM. The success in preparing Cd double-decker nanocrystals was further confirmed by the elemental signatures of C, Ce, N, Cl, and Cd in the energy-dispersive X-ray analysis spectrum as shown in Fig. 5. It is noteworthy that the observation of the O elemental signature in the spectrum is due either to the oxidized copper grids or to H_2O acting as one of ligands in the formed nanoscaled coordination polymers.

3.4. FT-IR spectra

FT-IR spectroscopy is a powerful method to study the coordination interaction between the double-decker compound and metal cations [53,54]. As shown in Fig. 6, except the decreased intensity, almost all the vibration bands observed in the IR spectrum of bulk double-decker compound can be found in the spectrum of Hg-[Ce(Pc)(TPyP)] nanowires. It is worth noting that the intense band appears at approximately 1592 cm^{-1} for the bulk double-decker molecules due to the C=N band vibration ($\nu_{C=N}$) of pyridyl substituents attached at the double-decker molecules, which shifts to 1602 cm^{-1} as a weak band in Hg-[Ce(Pc)(TPyP)] nanowires, indicating the formation of coordination bonds between N atoms of the pyridyl substituents of Ce(Pc)(TPyP) and Hg^{2+} cations. The intense band at 1330 cm^{-1} observed for both bulk double-decker com-

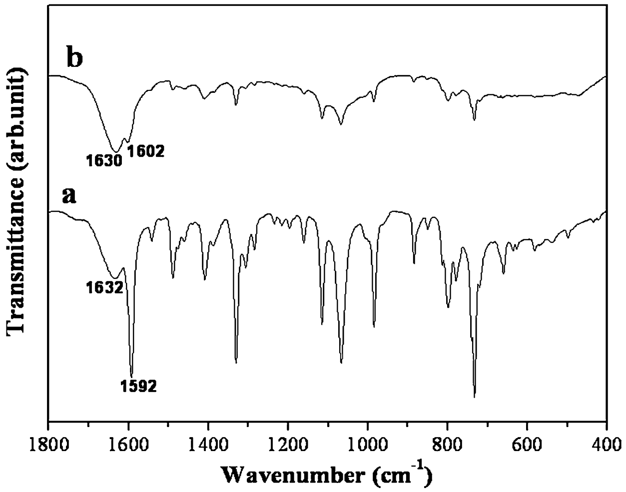

Fig. 6. FT-IR spectra of Ce(Pc)(TPyP) (a) and Hg–Ce(Pc)(TPyP) nanowires (b) in the region of 400–1800 cm^{-1} with 2 cm^{-1} resolution.

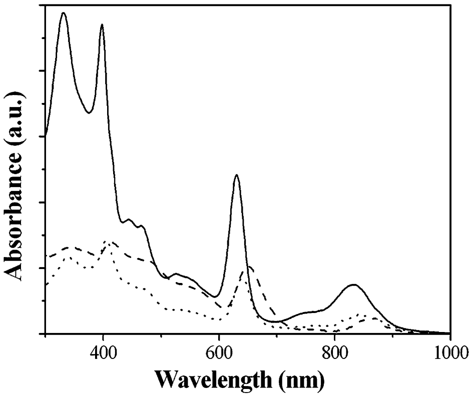

Fig. 7. Electronic absorption spectra of Ce(Pc)(TPyP) in $CHCl_3$ (—), LB films (···), and nanocrystals (- - -).

Table 1
UV–vis spectroscopic data for double-deckers [Ce(Pc)(TPyP)]

		λ_{max} (nm)
[Ce(Pc)(TPyP)]	$CHCl_3$ solution	331, 398, 633, 832
[Ce(Pc)(TPyP)]	LB films	340, 405, 643, 841
[Ce(Pc)(TPyP)]	Hg nanocrystal	348, 415, 652, 871

pound and Hg-mediated double-decker nanowires is the marker band of the phthalocyanine dianion [55,56].

3.5. UV–vis absorbance spectroscopy of metal-mediated double-decker Ce(Pc)(TPyP) nanocrystals

The electronic absorption spectra for the double-decker compound Ce(Pc)(TPyP) in $CHCl_3$, Langmuir–Blodgett films prepared from pure water surface, and Langmuir–Blodgett films of metal-mediated nanocrytals of Hg-[Ce(Pc)(TPyP)] transferred onto the hydrophobic quartz substrate surface after 1 day of interfacial reaction are compared in Fig. 7 and Table 1. In dilute chloroform solution, where the double-decker Ce(Pc)(TPyP) molecules are in monomer form, the spectrum shows strong Pc and TPyP Soret bands at 331 and 398 nm and a Pc Q band at 633 nm. In Langmuir–Blodgett films, where the Ce(Pc)(TPyP) molecules are in the form of aggregates, the Soret bands of Pc and TPyP are red-shifted to 340 and 405 nm and the Q band of Pc red-shifted to 643 nm. But in Hg^{2+}-mediated aggregates of Ce(Pc)(TPyP) formed at the interface of water and chloroform, all the Soret or Q bands mentioned above further red-shifted to 348, 415, and 652 nm, respectively. The red shift can be ascribed to the formation of J aggregates in LB film or in metal-mediated aggregates due to the π–π interaction [57]. The significant red shifts indicate strong π–π interactions between tetrapyrrole rings. This observation is remarkably different from that for metal-mediated monomeric H_2TPyP nanocrystal films. According to Qian and co-workers [47], the supramolecular interaction between porphyrin rings in the LB films of metal-mediated aggregates of H_2TPyP is stronger than that in solution but weaker than that in LB films. Our results provide an alternative way to increase the interactions between neighboring molecules in solid films when the intermolecular interaction is necessary.

4. Conclusions

In summary, sandwich-type mixed (phthalocyaninato) (porphyrinato) cerium double-decker compound was used as building blocks, for the first time, to fabricate into nanocrystals by metal-mediated assembly at the water–chloroform interface. Various morphologies of well-defined nanocrystals were formed depending on the varieties and concentration of metal cations: regular square nanocrystals were formed for Cd^{2+} cation and nanowires for Hg^{2+} cation. However, as far as Ag^{+} cation was concerned, two different morphologies, nanorods and regular quadrate, formed at the water–chloroform interface. It has been revealed that the geometries and the coordination mode of corresponding metal ions dominate the framework of coordination polymer nanocrystals formed. J-aggregates of the double-decker molecules formed in nanowire polymer films mediated by Hg^{2+} cation, which, however is different from that formed by monomeric H_2TPyP. These novel nanocrystals obtained are expected to be useful in the field of nanoelectronics.

Acknowledgments

Financial support from the Natural Science Foundation of China (Grants 20325105 and 20431010), National Ministry of Science and Technology of China (Grant 2001CB6105-07), Ministry of Education of China, and Shandong University is gratefully acknowledged.

References

[1] J.-M. Lehn, Supramolecular Chemistry: Concepts and Perspectives, VCH, Weinheim, 1995.
[2] D. Philp, J.F. Stoddart, Angew. Chem. 108 (1996) 1242–1286.
[3] D. Philp, J.F. Stoddart, Angew. Chem. Int. Ed. 35 (1996) 1155–1196.
[4] P. Samori, A. Fechtenkotter, F. Jackel, T. Bohme, K. Müllen, J.P. Rabe, J. Am. Chem. Soc. 123 (2001) 11,462–11,467.
[5] L. Zheng, J. Li, J. Phys. Chem. B 109 (2005) 1108–1112.
[6] O.D. Velev, K. Furusawa, K. Nagayama, Langmuir 12 (1996) 2374–2384.

[7] H. Jensen, J. Kakkassery, H. Nagatani, D. Fermin, H. Girault, J. Am. Chem. Soc. 122 (2000) 10,943–10,948.
[8] Y. Lin, H. Skaff, T. Emrick, A. Dinsmore, T. Russell, Science 299 (2003) 226–229.
[9] B. Su, J.-P. Abid, D.J. Fermín, H.H. Girault, H. Hoffmannova, P. Krtil, Z. Samec, J. Am. Chem. Soc. 126 (2004) 915–919.
[10] A. Kumar, S. Mandal, S.P. Mathew, P.R. Selvakannan, A.B. Mandale, R.V. Chaudhari, M. Sastry, Langmuir 18 (2002) 6478–6483.
[11] S.D. Sathsye, K.R. Patil, D.V. Paranjape, A. Mitra, A.B. Mandale, Langmuir 16 (2000) 3487–3490.
[12] P.W. Wu, L. Gao, J.K. Guo, Thin Solid Films 408 (2002) 132–135.
[13] J.B. Li, Y. Zhang, L.L. Yan, Angew. Chem. Int. Ed. 40 (2001) 891–894.
[14] G. Lu, H. Chen, J.B. Li, Colloids Surf. A 215 (2003) 25–32.
[15] K. Lee, M. Kim, J. Hahn, J. Suh, I. Lee, K. Kim, S. Han, Langmuir 22 (2006) 1817–1821.
[16] M.A. Ratner, J. Jortner, M.A. Ratner (Eds.), Molecular Electronics, Blackwell Science, London, 1997, p. 5.
[17] P.G. Schouten, J.M. Warman, M.P. de Haas, M.A. Fox, H.-L. Pan, Nature 353 (1991) 736–737.
[18] C.Y. Liu, H.-L. Pan, M.A. Fox, A.J. Bard, Science 261 (1993) 897–899.
[19] C.L. Honeybourne, C.A.S. Hill, R.J. Ewen, M.S. Collings, W.C. Clarke, J. Phys. Chem. Solids 49 (1988) 1003–1008.
[20] Y. Bian, J. Jiang, Y. Tao, M.T.M. Choi, R. Li, A.C.H. Ng, P. Zhu, N. Pan, X. Sun, D.P. Arnold, Z.-Y. Zhou, H.-W. Li, T.C.W. Mak, D.K.P. Ng, J. Am. Chem. Soc. 125 (2003) 12257–12267.
[21] F.J. Kampas, K. Yamashita, J. Fajer, Nature 284 (1980) 40–42.
[22] Y. Harima, K. Yamashita, J. Phys. Chem. 89 (1985) 5325–5327.
[23] Z. Gryczynski, R. Paolesse, K.M. Smith, E. Bucci, J. Phys. Chem. 98 (1994) 8813–8816.
[24] Z. Bao, A.J. Lovinger, A. Dodabalapur, Adv. Mater. 9 (1997) 42–44.
[25] K. Xiao, Y. Liu, X. Huang, Y. Xu, G. Yu, D. Zhu, J. Phys. Chem. B 107 (2003) 9226–9230.
[26] J. Lochlin, K. Shinbo, K. Onishi, F. Kaneko, Z. Bao, R.C. Advincula, Chem. Mater. 15 (2003) 1404–1412.
[27] W. Su, J. Jiang, K. Xiao, Y. Chen, Q. Zhao, G. Yu, Y. Liu, Langmuir 21 (2005) 6527–6531.
[28] Y. Chen, W. Su, M. Bai, J. Jiang, X. Li, Y. Liu, L. Wang, S. Wang, J. Am. Chem. Soc. 127 (2005) 15,700–15,701.
[29] X.Q. Zhang, H.M. Wu, X.J. Wu, Z.P. Cheng, Y. Wei, J. Mater. Chem. 5 (1995) 401–404.
[30] J.H. Fendler, Membrane Mimetic Chemistry, Wiley, New York, 1982.
[31] D. Xie, Y. Jiang, J. Jiang, Z. Wu, Y. Li, Sens. Actuat. B 77 (2001) 260–263.
[32] D. Battisti, R. Aroca, J. Am. Chem. Soc. 114 (1992) 1201–1204.
[33] Y. Chen, H. Liu, N. Pan, J. Jiang, Thin Solid Film 460 (2004) 279–285.
[34] R.S. Lokey, B.L. Iverson, Nature 375 (1995) 303–305.
[35] J.C. Nelson, J.G. Saven, J.S. Moore, P.G. Wolynes, Science 277 (1997) 1793–1796.
[36] H. Engelkamp, S. Middelbeek, R.J.M. Nolte, Science 284 (1999) 785–788.
[37] M. Shirakawa, N. Fujita, S. Shinkai, J. Am. Chem. Soc. 125 (2003) 9902–9903.
[38] T. Kishida, N. Fujita, K. Sada, S. Shinkai, J. Am. Chem. Soc. 127 (2005) 7298–7299.
[39] C.V.K. Sharma, G.A. Broker, J.G. Huddleston, J.W. Baldwin, R.M. Metzger, R.D. Roger, J. Am. Chem. Soc. 121 (1999) 1137–1144.
[40] L. Carlucci, G. Ciani, D.M. Proserpio, F. Porta, Angew. Chem. Int. Ed. 42 (2003) 317–322.
[41] M. Kondo, Y. Kimura, K. Wada, T. Mizutani, Y. Ito, S. Kitagawa, Chem. Lett. (2000) 818–819.
[42] D.J. Qian, C. Nakamura, J. Miyake, Langmuir 16 (2000) 9615–9619.
[43] D.J. Qian, C. Nakamura, J. Miyake, Chem. Commun. (2001) 2312–2313.
[44] J.L. Ruggles, G.J. Foran, H. Tanida, H. Nagatani, Y. Jimura, I. Watanabe, I.R. Gentle, Langmuir 22 (2006) 681–686.
[45] Z.-Y. Yang, L.-H. Gan, S.-B. Lei, L.-J. Wan, C. Wang, J.-Z. Jiang, J. Phys. Chem. B 109 (2005) 19,859–19,865.
[46] S. Yoshimoto, K. Suto, A. Tada, N. Kobayashi, K. Itaya, J. Am. Chem. Soc. 126 (2004) 8020–8027.
[47] B. Liu, D.-J. Qian, H.-X. Huang, T. Wakayama, S. Hara, W. Huang, C. Nakamura, J. Miyake, Langmuir 21 (2005) 5079–5084.
[48] B. Liu, D. Qian, M. Chen, T. Wakayama, C. Nakamura, J. Miyake, Chem. Commun. (2006) 3175–3177.
[49] L. Qi, H. Cölfen, M. Antonietti, Chem. Mater. 12 (2000) 2392–2403.
[50] D. Zhang, L. Qi, J. Ma, H. Cheng, Chem. Mater. 13 (2001) 2753–2755.
[51] L. Qi, J. Ma, H. Cheng, Z. Zhao, J. Phys. Chem. B 101 (1997) 3460–3463.
[52] H. Cölfen, M. Antonietti, Langmuir 14 (1998) 582–589.
[53] Z. Zhang, T. Imae, Nano Lett. 1 (2001) 241–243.
[54] J. Yuan, M. Liu, J. Am. Chem. Soc. 125 (2003) 5051–5056.
[55] J. Jiang, M. Bao, L. Rintoul, D.P. Arnold, Coordin. Chem. Rev. 250 (2006) 424–448.
[56] R. Wang, R. Li, Y. Li, X. Zhang, P. Zhu, P. Lo, D.K.P. Ng, N. Pan, C. Ma, N. Kobayashi, J. Jiang, Chem. Eur. J. 12 (2006) 1475–1485.
[57] A.W. Snow, in: K.M. Kadish, K.M. Smith, R. Guilard (Eds.), The Porphyrin Handbook, Elsevier, Amsterdam, 2003, p. 129.